Self-consistent mean-field calculation of surface segregation in a binary polymer blend

J. Genzer, A. Faldi, and R. J. Composto

*Department of Materials Science and Engineering and Laboratory for Research on the Structure of Matter, University of Pennsylvania,
Philadelphia, Pennsylvania 19104-6272*
(Received 20 May 1994)

In this Brief Report we use a self-consistent mean-field (SCF) method to predict the surface excess (z^*) and surface volume fraction (ϕ_1) of the surface active component in a binary polymer blend. The SCF results are in excellent agreement with the measured z^* and ϕ_1 values of deuterated polystyrene (dPS) in a blend of dPS and PS. However, the approach proposed by Schmidt and Binder (SB) [J. Phys. (Paris) **46**, 1631 (1985)] fails to predict simultaneously z^* and ϕ_1 for the same value of the excess surface free energy. A comparison of the dPS volume fraction profiles calculated by the SCF and SB models illustrates the limitations of the SB theory as applied to the dPS-PS experiments. Using the SCF model, the excess surface free energy is shown to have a complex dependence on ϕ_1, in contrast to the linear behavior proposed by SB.

The wetting of an interface by a binary fluid mixture, first described by Cahn [1] in 1977, has been recently extended to a binary polymer mixture [2,3]. Because a free surface can introduce a preferential attraction for one component, the surface becomes enriched with this species, whose volume fraction profile is determined by the surface-segment interaction and the bulk free energy of mixing. This volume fraction profile decays monotonically from its surface value to its bulk value over a distance on the order of the radius of gyration of the segregated polymer. Using forward recoil spectrometry, neutron reflectivity, time-of-flight forward recoil spectrometry, and secondary ion mass spectrometry, Jones and co-workers showed that the surface region of a mixture of high-molecular-weight polystyrene (PS) and its deuterated counterpart (dPS) is enriched by dPS, the component with the lower surface energy [4,5]. The mean-field theory introduced by Schmidt and Binder [3] (SB) was used to describe these and other experimental data [4–6]. In a recent publication, Shull suggested that the self-consistent field (SCF) approach is a powerful tool for investigating surface segregation from a binary mixture of two homopolymers [7].

In this Brief Report we apply the SCF method to calculate the volume fraction profile in an *A-B* polymer blend. In particular, the surface volume fraction and surface excess of the segregated species (i.e., *A*) predicted by this method are in excellent agreement with experimental values. We also show that the SB model provides only a qualitative description of the surface segregation. The deviations are explained in terms of assumptions inherent to the SB approach.

Our SCF calculations follow the framework developed by Hong and Noolandi, and Shull [7–9]. These calculations are based on the distribution functions $q_k(x,t)$, which represent the probability that the tth segment of polymer k is at a distance x from the chain end. The distribution functions are solutions to the modified diffusion equation [10]:

$$\frac{\partial q_k(x,t)}{\partial t} = R_{g,k}^2 \frac{\partial^2 q_k(x,t)}{\partial x^2} - \frac{N_k}{k_B T} w_k(x) q_k(x,t) , \quad (1)$$

where $R_{g,k}$ is the radius of gyration of polymer k, N_k is the number of segments of polymer k, k_B is Boltzmann's constant, and T is the absolute temperature. The influence of a weakly perturbing mean field $w_k(x)$ on polymer A is given by [7–9]

$$\frac{w_A(x)}{k_B T} = \frac{1}{N_A k_B T}[\mu_A(x) - \mu_{A,\infty}]$$
$$- \frac{\ln\phi_A(x)}{N_A} - \frac{\Delta w(x)}{k_B T} - \frac{w_{A,\text{ext}}(x)}{k_B T}, \quad (2)$$

where $\mu_A(x)$ and $\mu_{A,\infty}$ are the chemical potentials of the polymer A at position x and in the bulk, respectively, and ϕ_A is the volume fraction of polymer A. Using the Flory-Huggins free energy density to express the chemical potentials, Eq. (2) becomes

$$N_A \frac{w_A(x)}{k_B T} = \phi_{A,\infty} - \ln\phi_{A,\infty} + \left[\frac{R_{g,A}}{R_{g,B}}\right]^2 \phi_{B,\infty}$$

$$- \chi N_A[\phi_{B,\infty}^2 - \phi_B^2(x)]$$

$$- \left[\phi_A(x) - \left[\frac{R_{g,A}}{R_{g,B}}\right]^2 \phi_B(x)\right]$$

$$- N_A \frac{\Delta w(x)}{k_B T} - N_A \frac{w_{A,\text{ext}}(x)}{k_B T}. \quad (3)$$

Here, ϕ_k and $\phi_{k,\infty}$ are the volume fraction and bulk volume fraction of polymer k, respectively, and χ is the Flory-Huggins interaction parameter. As discussed elsewhere [9], the term $\Delta w(x)$ is introduced to enforce incompressibility of the mixture, i.e., $\phi_A + \phi_B = 1$. The expression for $\Delta w(x)$ is

$$\Delta w(x) = \zeta \left[1 - \sum_k \phi_k(x) \right] , \tag{4}$$

where ζ is proportional to the bulk compressibility of the mixture [11]. Empirically, $\zeta = 5$ provides a good compromise between stability and rate of convergence of the SCF calculations. The calculated volume fraction profile is independent of the value of ζ providing the calculation converges. The influence of the surface on polymers A and B is introduced via the external field $w_{A,\text{ext}}(x)$. Because we consider an incompressible mixture, it is sufficient to consider the difference between the surface fields acting on polymers A and B [9]. Thus, $w_{A,\text{ext}}(x)$ represents the free energy gain associated with the replacement at the surface of a B segment with an A segment, and has the form [9]

$$N_A \frac{w_{A,\text{ext}}(0)}{k_B T} = \frac{6 R_{g,A}^2}{a^3} \left[-\frac{df_S}{d\phi_{A,1}} \right] , \tag{5}$$

where f_S is the "bare" surface energy, $\phi_{A,1}$ is the surface volume fraction of A, and a is the polymer segment length, assumed to be the same for A and B $(R_{g,A}^2 = a^2 N_A / 6)$. The term $-df_S/d\phi_{A,1}$ represents the driving force for segregation and throughout this article is called the excess surface free energy. Following previous studies [2,3,7,9], we consider a short-range interaction between the polymers and the surface. Thus, only segments within a distance a of the surface are influenced by the external surface field [Eq. (5)]. Within the SCF framework, we have shown [12] that the addition of long-range interactions has a minor effect on the calculated volume fraction profile. Long-range interactions will be discussed in a future paper [13].

Self-consistent solutions to Eqs. (1)–(5) are obtained by the following procedure: Starting with a choice of $-df_S/d\phi_{dPS,1}$ and an initial assumption for the concentration profiles $\phi_A(x)$ and $\phi_B(x)$, Eq. (1) is solved simultaneously for both polymers using appropriate initial and boundary conditions [8]. Using these values of $q_k(x,t)$, new concentration profiles are calculated and serve as the new input for the next calculation of the distribution functions. This procedure is repeated until the two subsequent iterations, given by n and $n+1$, satisfy the following condition:

$$\max_{(x,k)} |w_k^{(n+1)}(x) - w_k^{(n)}(x)| \le 10^{-4} . \tag{6}$$

The SCF predictions were compared with Zhao et al.'s measurements [5] on blends of dPS and PS having weight-average molecular weights of 1.03×10^6 and 1.8×10^6 g/mol, respectively. Although other measurements exist [4], we believe that Zhao et al.'s data correspond to the equilibrium state of the system. Blends of PS and dPS were annealed in the one-phase region of the phase diagram at 184 °C, a temperature which corresponds to $\chi = 1.5 \times 10^{-4}$ [14]. Using secondary ion mass spectrometry (SIMS), the surface excess z_{dPS}^* and the surface concentration $\phi_{dPS,1}$ of dPS were determined as a function of the bulk volume fraction of dPS, $\phi_{dPS,\infty}$.

In Eqs. (1)–(5), polymers A and B correspond to dPS and PS, respectively. To decrease the computation time, we use values of N_{dPS} and N_{PS} which are smaller than the degrees of polymerization of the "real" polymers (the first row in Table I) used in the experiments. Scaling is accomplished by choosing different values of a, while always maintaining the same $R_{g,dPS}$, $R_{g,PS}$, χN_A, mass densities, and chain volumes of the polymers. The values of the molecular parameters of the "scaled" polymers used in the calculations are reported in Table I (second and third rows). It is apparent that the above procedure leaves Eqs. (1)–(5) unchanged except for the external field term [15]. For each $\phi_{dPS,\infty}$ we choose, by trial and error, the $-df_S/d\phi_{dPS,1}$ that minimizes the difference between the calculated z_{dPS}^* and $\phi_{dPS,1}$ and their experimental values. Clearly, $-df_S/d\phi_{dPS,1}$ depends on the chosen value of a [see Eq. (5)], and it can be shown [13] that $-df_S/d\phi_{dPS,1} \sim a^2$. It will be demonstrated that a single value of $-df_S/d\phi_{dPS,1}$ produces z_{dPS}^* and $\phi_{dPS,1}$ values in excellent agreement with the experimental values.

Figure 1 shows (a) the surface excess z_{dPS}^* and (b) the surface concentration $\phi_{dPS,1}$ of dPS as a function of $\phi_{dPS,\infty}$. The solid circles and solid lines represent values determined by SIMS [5] and the SCF model, respectively. According to Ref. [5], the experimental errors in z_{dPS}^* and $\phi_{dPS,1}$ are less than the size of the symbols. Using a single value of the excess surface free energy for each bulk concentration, the SCF results provide an excellent fit to the experimental values of z_{dPS}^* and $\phi_{dPS,1}$. The dotted line in Fig. 1(a) is the result of the SB model calculated from [3,4]

$$z_{dPS}^* = \frac{a}{6} \int_{\phi_{dPS,1}}^{\phi_{dPS,\infty}} \frac{(\phi - \phi_{dPS,\infty}) d\phi}{\sqrt{\{\phi(1-\phi)[G(\phi) - G(\phi_{dPS,\infty}) - \Delta\mu(\phi - \phi_{dPS,\infty})]\}}} \tag{7}$$

using the experimentally determined $\phi_{dPS,1}$. In Eq. (7), G is the Gibbs free energy of mixing per lattice site and $\Delta\mu$ is the exchange chemical potential $(\partial G/\partial \phi)$. Although the SB model is in qualitative agreement with experiments, it underestimates the experimental values of z_{dPS}^* by up to ca. 20%. This observation shows that one cannot fit both z_{dPS}^* and $\phi_{dPS,1}$ simultaneously using the SB

model. The dashed line in Fig. 1(b) represents the SB prediction for $\phi_{dPS,1}$ calculated from the experimental data for z_{dPS}^* using Eq. (7). Similar to Fig. 1(a), the trend of the functional dependence of $\phi_{dPS,1}$ on $\phi_{dPS,\infty}$ is the same for both the SCF and the SB models, but SB overestimates the values of $\phi_{dPS,1}$. In contrast to the SCF approach, it is evident from Fig. 1 that the SB method can-

TABLE I. Molecular parameters of the dPS-PS system. The values in row 1 denote parameters for the dPS and PS used in the experiments. The values in rows 2 and 3 represent the scaled parameters used in the SCF calculations. M_0 is the molecular weight of a segment.

a (nm)	N_{dPS}	N_{PS}	$M_{0,dPS}$ (g/mol)	$M_{0,PS}$ (g/mol)	$10^4\chi$
0.67	9190	17 300	112	104	1.5
1.20	2865	5 393	359	334	4.8
1.40	2105	3 963	489	454	6.6

not fit both z^*_{dPS} and $\phi_{dPS,1}$ simultaneously.

The volume fraction profile of dPS calculated for $\phi_{dPS,\infty} = 0.105$ is shown in Fig. 2. The solid and dashed lines represent the SCF and SB profiles calculated for $z^*_{dPS} = 0.9$ nm. Notice that $\phi_{dPS,1}$ is larger in the SB profile, in agreement with Fig. 1(b). When one constrains

FIG. 2. Calculated volume fraction profiles in a dPS-PS blend having $\phi_{dPS,\infty} = 0.105$. The solid and dashed lines are calculated using the SCF and the SB [3] models, respectively. Both curves have $z^*_{dPS} = 9.8$ nm. The dotted line represents the SB profile that has the same $\phi_{dPS,1}$ as the SCF profile. All the line types coincide with those from Fig. 1.

the SB volume fraction profile to have the same $\phi_{dPS,1}$ as the SCF profile, the surface excess of the SB profile is lowered, as is apparent from the dotted line shown in Fig. 2. Therefore, we reach the same conclusion as is drawn from Fig. 1—namely, that the SCF model can profile a more precise description of the volume fraction profile of the segregated species than the SB approach.

The values of $-df_S/d\phi_{dPS,1}$ used in the SCF calculations are plotted in Fig. 3 as a function of the measured $\phi_{dPS,1}$. As explained previously, the values of $-df_S/d\phi_{dPS,1}$ are chosen such that the SCF and experimental values of z^*_{dPS} and $\phi_{dPS,1}$ are in good agreement. The calculations were performed with $a = 1.2$ and 1.4 nm and the results were scaled to $a = 0.67$ nm. Obviously, the form suggested by Schmidt and Binder [3],

$$-\frac{df_S}{d\phi_{dPS,1}} = \mu_1 + g\phi_{dPS,1} , \tag{8}$$
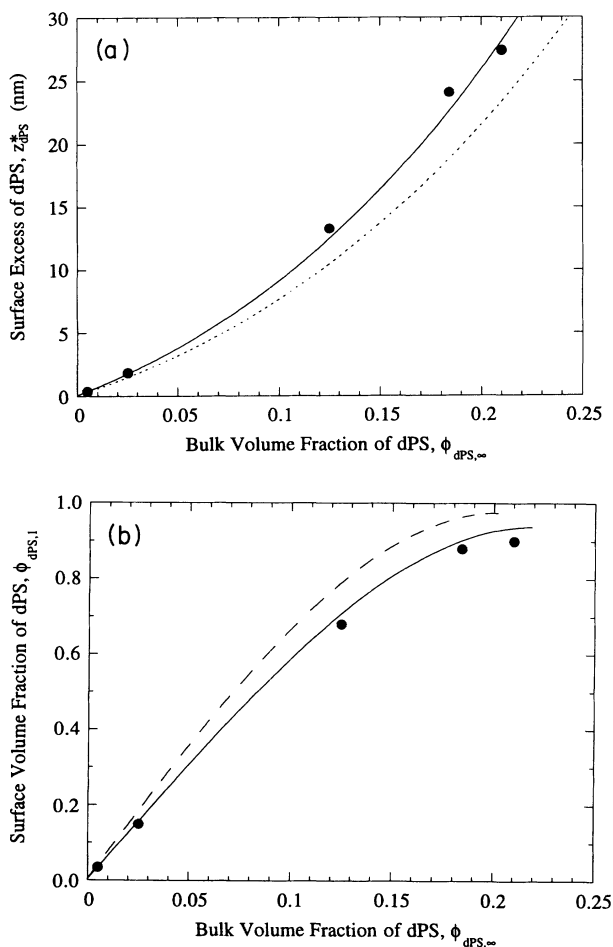

FIG. 1. (a) Surface excess of dPS, z^*_{dPS}, as a function of the volume fraction of dPS in the bulk, $\phi_{dPS,\infty}$. The solid circles represent data measured using SIMS [5]. The solid and dotted lines were calculated using the SCF and the SB [3] models, respectively. (b) Volume fraction of dPS at the surface, $\phi_{dPS,1}$, as a function of the volume fraction of dPS in the bulk, $\phi_{dPS,\infty}$. The solid circles represent data determined by SIMS [5]. The solid and dashed lines were calculated using the SCF and the SB [3] models, respectively.
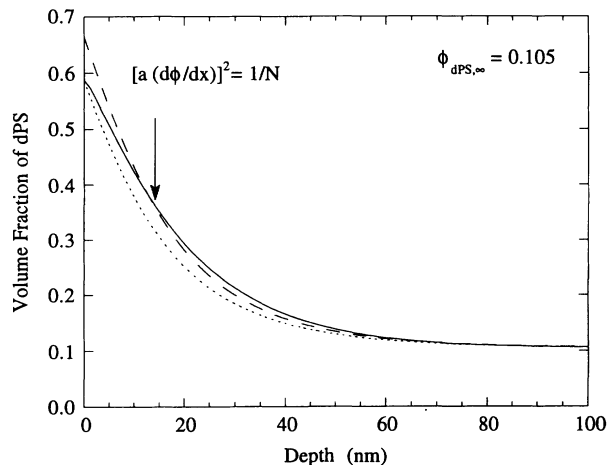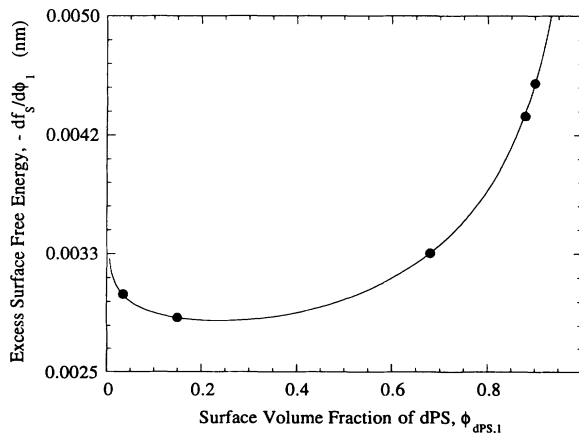

FIG. 3. Excess surface free energy used in the SCF calculations as a function of the measured surface volume fraction of dPS. The solid line is a guide to the eye.

fails to describe the functional dependence of $-df_S/d\phi_{\text{dPS},1}$. Here, μ_1 is the chemical potential difference that favors the dPS component at the surface and g is related to the interaction of the segments of dPS and PS at the surface. The dependence of $-df_S/d\phi_{\text{dPS},1}$ on $\phi_{\text{dPS},1}$ shown in Fig. 3 is in qualitative agreement with calculations deduced from the same experiments [5] using Schmidt and Binder's theory, although the former values are about 30% higher. Recently, new expressions for $-df_S/d\phi_{\text{dPS},1}$ have been proposed [16,17]. In particular, the functional form proposed by Cohen and Muthukumar [16] was used by Zhao et al. [5] to obtain a reasonable fit to the experimental values of $-df_S/d\phi_{\text{dPS},1}$. A detailed analysis of the functional form for the "bare" surface energy will be discussed in a future paper [13].

The preceding discussion highlights the limitations of the SB model as applied to the high-molecular-weight blend of dPS and PS. One limitation of the SB approach, clearly stated in Ref. [3], is that the theory is valid when

$$a^2 \left| \frac{d\phi}{dx} \right|^2 \ll \frac{1}{N} . \tag{9}$$

The arrow in Fig. 2 delimits the surface region (ca. 14 nm) over which the volume fraction profile varies too sharply to satisfy Eq. (9). Note that the discrepancy between the SB (dashed) and SCF (solid) profiles is largest between the surface and about 14 nm. Although the SCF model remains valid when the profile curvature is large, it must be applied to polymer chains long enough that any influence of the discretization involved in the numerical

solution of Eq. (1) becomes negligible [18]. Like all mean-field approaches, the SCF model is not valid in the vicinity of the critical point because it neglects critical fluctuations.

In conclusion, we have shown that the SCF approach can accurately predict the surface excess and the surface volume fraction of the segregated species in blends of high-molecular-weight polystyrene and deuterated polystyrene. In contrast to the SCF model, the SB theory fails to predict simultaneously both the surface excess and the surface volume fraction of dPS determined experimentally. The discrepancy between the SCF and SB models may be due to approximations inherent in the latter approach. The dependence of the excess surface free energy on the surface volume fraction predicted by the SCF model is in qualitative agreement with the values determined from experiments. This result also supports the validity of the SCF approach.

[1] J. W. Cahn, J. Chem. Phys. **66**, 3667 (1977).

[2] H. Nakanishi and P. Pincus, J. Chem. Phys. **79**, 997 (1983).

[3] I. Schmidt and K. Binder, J. Phys. (Paris) **46**, 1631 (1985).

[4] R. A. L. Jones et al., Phys. Rev. Lett. **62**, 280 (1989); Europhys. Lett. **12**, 41 (1990); J. Sokolov et al., Appl. Phys. Lett. **54**, 590 (1989); R. J. Composto et al., Physica B **156&157**, 434 (1989); M. H. Rafailovich et al., Hyperfine Interactions **62**, 45 (1990).

[5] X. Zhao et al., Macromolecules **24**, 5991 (1991).

[6] See, for example, A. Budkowski, U. Steiner, and J. Klein, J. Chem. Phys. **97**, 5229 (1992); F. Bruder and R. Brenn, Europhys. Lett. **22**, 707 (1993); J. M. G. Cowie, B. G. Devlin, and I. J. McEwen, Macromolecules **26**, 5628 (1993).

[7] K. R. Shull, Macromolecules **26**, 2346 (1993).

[8] K. M. Hong and J. Noolandi, Macromolecules **14**, 727 (1981); K. R. Shull and E. J. Kramer, ibid. **23**, 4769 (1990).

[9] K. R. Shull, J. Chem. Phys. **94**, 5723 (1991); Macromolecues **25**, 2122 (1992).

[10] S. A. Edwards, Proc. Phys. Soc. London **85**, 613 (1965).

[11] E. Helfand and Y. Tagami, Polym. Lett. **9**, 741 (1971).

[12] J. Genzer, A. Faldi, and R. J. Composto, Bull. Am. Phys. Soc. **39**, 570 (1994). Our result is also in accord with a recent study by Jones, Phys. Rev. E **47**, 1437 (1993).

[13] J. Genzer, A. Faldi, and R. J. Composto (unpublished).

[14] F. S. Bates and G. D. Wignall, Phys. Rev. Lett. **57**, 1429 (1986).

[15] The term $\Delta w(x)$ is nearly zero at the end of each simulation.

[16] S. M. Cohen and M. Muthukumar, J. Chem. Phys. **90**, 5749 (1989).

[17] R. A. Jerry and E. B. Nauman, J. Coll. Interface Sci. **154**, 122 (1992); J. Chem. Phys. **97**, 7829 (1992); Phys. Lett. A **167**, 198 (1992); Phys. Rev. E **48**, 1583 (1993).

[18] This condition is satisfied for N larger than ~ 500. Details will be given in Ref. [13].